

Ozonolysis in Flow Using Capillary Reactors

M. D. Roydhouse,[†] A. Ghaini,[‡] A. Constantinou,[‡] A. Cantu-Perez,[‡] W. B. Motherwell,[†] and A. Gavriilidis^{*,‡}

[†]Department of Chemistry, University College London, 20 Gordon Street, London WC1H 0AJ

[‡]Department of Chemical Engineering, University College London, Torrington Place, London WC1E 7JE

ABSTRACT: Reactions of *n*-decene with ozone and subsequent quenching of the formed ozonides were carried out under flow conditions using the standard Vapourtec flow system equipped with a cooled flow cell. The reactions were performed continuously and in the annular flow regime within the circular cross-section channels. Typical flow rates were 0.25–1 mL min⁻¹ for liquid and 25–100 mL min⁻¹ for gas, reactor volumes were 0.07–10 mL formed of 1 mm ID PFA tubing. The reaction temperature was –10 °C. The flow was not always smooth, while waves in the liquid film and droplets in the gas core were observed. Liquid residence times were found to be independent of gas flow rates and increasing with decreasing liquid flow rates. Substrate residence times in the ozonolysis reactor ranged between 1 and 80 s, and complete conversion could be achieved at ~1 s residence time. Two common reductants, triethylphosphite and triphenylphosphine, were examined as to their suitability under flow conditions. Triphenylphosphine achieved faster reduction of the intermediate ozonides, resulting in a greater than 10:1 selectivity for the aldehyde over the corresponding acid. The cooling system provided a safe and efficient control of the highly exothermic reaction system. The configuration of the system allowed the production of chemically significant amounts (1.8 g h⁻¹ at 1.3 ozone equivalents), with minimal amounts of ozonides present at any time.

INTRODUCTION

Ozone is an oxidant that has been used for decades in organic synthesis¹ and in the purification/deodorisation of water.² Ozonolysis is the addition of ozone to a substance, resulting initially in a primary ozonide which then usually rearranges to a more stable secondary ozonide in the case of alkenes.³ The most common substrates for ozonolysis are unsaturated species containing either double or triple carbon–carbon bonds, which result usually in aldehydes/ketones and acids. This transformation has great utility in synthesis both in a research and an industrial setting. Ozone can also be used to oxidise phosphorus^{1,4} and sulphur^{1,5} compounds as well as organometallics⁶ and other inorganic species.⁶ The advantages of using ozone over other oxidants is the low cost and toxicity of the byproduct, i.e. DMSO from DMS, Ph₃PO from PPh₃ as compared with high oxidation level metallic oxidants, e.g. chromium. Some of the drawbacks of using ozone at scale are the high exotherms associated with the initial reaction of substrates with ozone.⁷ Also the intermediate ozonides are unstable (although some can be isolated at room temperature) and are an explosion risk due to the instability of the O–O single bond; the build-up of these materials must be avoided. The use of continuous flow can alleviate both the exotherm problem and the build-up of potentially explosive materials (if suitable reagents are used to quench them in flow).

Microreactors have shown several benefits in the past years. Microstructured devices provide short diffusion pathways, improved heat and mass transfer rates, and increased contact areas for two-phase reaction systems.⁸ Additionally, the small dimensions allow safer handling of hazardous materials and continuous processing. Microreactors for ozonolysis reactions were first used by Wada et al.⁹ Oxidation of organic substrates were performed by using multichannel microreactors fabricated from silicon and Pyrex wafers. Microfabricated posts within the reactor channels were found to enhance mass transfer. Triethyl phosphite, octylamine,

and 1-decene were oxidized at liquid flow rates of ~0.05 mL min⁻¹ and a liquid to gas ratio of 1:100 in the annular-flow regime. Contact times as low as 1 s and conversions and selectivities up to 100% were reported. Falling film microreactors have also been used to perform ozonolysis reactions.^{10–12} Olefin conversions were shown to increase with increasing liquid-phase residence times, while an increase in the gas flow rates resulted in ozone absorption rates up to 1.9 × 10⁻³ mol s⁻¹. Temperature did not show an influence on the selectivity. Other types of microreactors have also been evaluated: a cyclone mixer and five-channel mixer made by Mikroglas.¹² The channel mixer showed better performance than the falling film microreactor. Recently, the Ley group have shown an ozonolysis reaction utilizing a semipermeable membrane capillary.¹³ The semipermeable tube, consisting of an amorphous copolymer of tetrafluoroethylene and perfluorodimethyldioxolane, allows gas but not liquid to cross the membrane. The microporous structure has high gas permeability. Full conversion of various alkenes could be reached at residence times of about 1 h.

A number of experimental factors can affect two-phase flow within a channel, and numerous flow patterns such as segmented flow, bubbly flow, or annular flow can be present.¹⁴ In the annular two-phase flow pattern the liquid phase flows in a film adjacent to the wall surface. At high gas velocity large amplitude flow surges appear in the film.^{15,16} These disturbance waves, noted as a key mechanism of heat and mass transfer, are characterized by coherent motion over several tube diameters.¹⁷ Above a critical liquid flow rate, a significant portion of the input liquid feed can exist as droplets entrained in the gas core. The droplets form from the disturbance waves, accelerate in the gas core, and deposit back onto the film. This process increases the overall pressure drop of

Received: February 9, 2011

Published: June 23, 2011

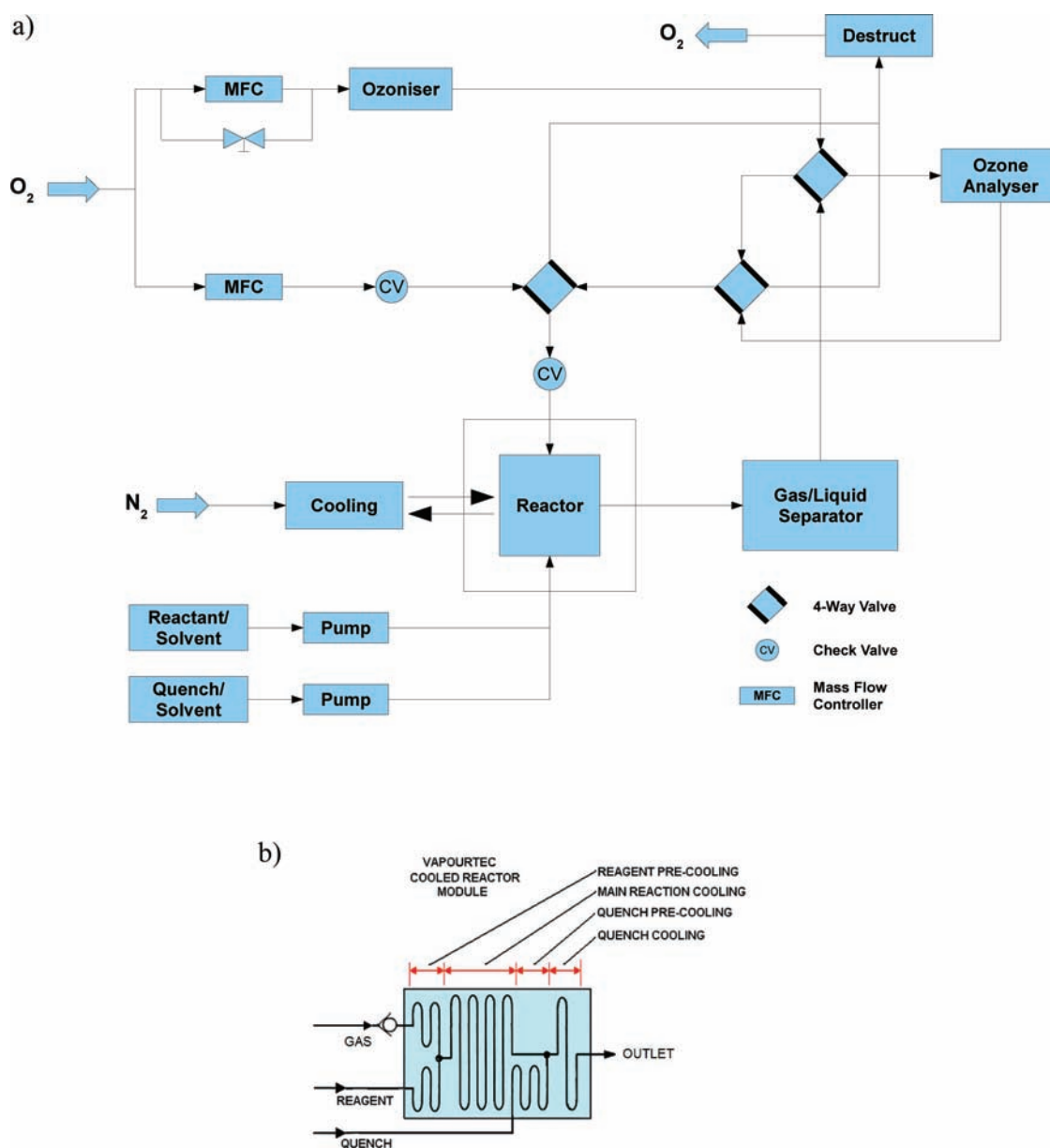


Figure 1. (a) Schematic of ozonolysis setup, (b) schematic of Vapourtec cooled reactor module.

the system and enhances heat and mass transfer above that expected in single flows.¹⁸

EXPERIMENTAL SECTION

Flow Reactor Setup. The Vapourtec R4 system is a widely established piece of equipment in an industrial R&D setting and has many uses in liquid phase procedures. Most R&D centres also have access to an ozoniser. The coupling of these relatively common pieces of equipment as demonstrated in this paper gives many advantages over a purpose-built system; these are modularity, low cost, versatility, and simplicity. The Vapourtec R4 flow system was used with a cooled flow cell, capable of being cooled to -70 °C via an inert gas stream chilled over dry ice. The required ozone was provided via a BMT 803 HP ozoniser fed with pure oxygen. Ozone was measured with a BMT 964 analyser. A schematic of the setup is shown in Figure 1.

The initial oxygen gas stream (BOC Oxygen >99.5%) at 2 bar was split into two, with one being fed via a thermal mass flow controller (Brooks 4800) and $0.5 \mu\text{m}$ particle filter to the ozoniser, the other blank oxygen stream being controlled via a mechanical mass flow controller. Both streams then enter a system of three four-way valves to which the flow reactor and ozone analyser are connected, while check-valves are placed at two positions to avoid any backflow (see Figure 1 for more details on connections). This arrangement allows multiple configurations. Two principle configurations are the ozone analyser placed either upstream or downstream of the reactor module, resulting in the ability to measure the ozone concentrations before and after the reactor. In this work the ozone analyser was placed in between the ozoniser and the reactor. Other configurations allow the safe isolation of the reactor module and/or analyser. The off-gases pass from the reactor module and through the four-way valve system to a catalytic destructor consisting of a 100-mL volume 316 stainless steel cartridge loaded

Table 1. Ozonolysis flow setup operating parameters

parameter	range
reactor volume	0.07, 2, 5, 10 mL
reactor internal diameter	1 mm
gas flow rate	25–66 mL min ⁻¹
reactant flow rate	0.25–1.08 mL min ⁻¹
quench flow rate	0.25–1.44 mL min ⁻¹
temperature	–10 °C
pressure	1.1–1.3 bar (reactor inlet)

with Carus Carulite 200 (manganese dioxide/copper oxide). The efficiency of the catalyst is checked on a regular basis by bubbling the treated gases through 10% potassium iodide solution. The presence of ozone would be immediately detected by the formation of dark brown iodine.

The concentration of ozone at the outlet of the ozone generator is dependent on the electric power consumption, gas flow rate, and temperature. The dielectric is plain ceramic, and the electrodes are tungsten with a maximum operating pressure of 2 bar gauge. The ozone concentration can reach ~280 g/Nm³ (~19 wt %), depending on the power setting, with the maximum concentration being reached around setting 6 (scale 1–10); higher power settings result in a lower yield of ozone. At flow rates below 25 mL min⁻¹, the ozone concentration was found to be unacceptably variable and therefore unusable. The ozone analyser measures the ozone content with a UV photometer at a wavelength of 254 nm, and the maximum operating pressure is 1 bar gauge.

The Vapourtec R4 cooled reactor module consists of three input streams (one after the main reactor cartridge) and one output stream (Figure 1b). All internal tubing is 1 mm ID PFA. The module is cooled via a stream of dried air chilled over dry ice and distributed internally via a fan. Temperature control is via a pinch valve controlled by the system. The ozone-containing oxygen gas stream, flowing through a nonreturn valve, is precooled on entry to the cooled reactor module (Figure 1b) and then mixed via a 1 mm ID “T” with the precooled substrate solution. The gas/liquid mixture then proceeds through a reactor cartridge. The cartridge consists of a weaved coil of circular PFA tubing with 1 mm ID, which gives a reactor volume of about 8.1 μL/cm. Volumes used were 0.07, 2, 5, and 10 mL. The cartridge ends at another 1 mm ID “T” where the gas/liquid stream is mixed with the precooled quench solution. A short, cooled tube of 500 mm length (0.39 mL) follows, allowing dissipation of any exotherm. The output gas/liquid mixture is separated by gravity in a PTFE-capped 50 mL bottle, where the liquid is collected at the bottom and the gas allowed to exit via a 2-mm ID tube to the four-way valve system. Ozone is highly aggressive to most plastics and rubbers and degrades these materials rapidly, while stainless steel (316), PTFE and PFA are ozone resistant. Therefore, all parts of the experimental setup that are in contact with either fluids or gas consist of either PTFE, PFA, or stainless steel (316). The connection tubes used in the setup are either 1/8 in. (3.18 mm) or 1/16 in. (1.15 mm) ID. The range of operating conditions used are shown in Table 1.

Hydrodynamics Characterisation. In order to characterise the gas/liquid behaviour, flow patterns, film thickness, and residence time were investigated. The flow patterns and the liquid film thickness of the gas/liquid mixture were analysed using a Phantom Miro 4 high-speed camera; the images were acquired at 200 pps. Straight PFA tubing with 1 mm ID and 10 cm length was used for the flow patterns and the liquid film thickness analysis. The gas/liquid

mixture was ethyl acetate/nitrogen. A syringe pump (Cole Parmer 74900–35) was used to deliver the liquid, while the gas was introduced by a mass flow controller (Brooks 5850). Gas and liquid were brought together by a PEEK Y-mixer with 1 mm ID. For residence time determination, coils of 2, 5, and 10 mL internal volume, as employed in the ozonolysis experiments, were used. Ethyl acetate containing a dye (Parker blue) was used in tracer step-input experiments. Signals from the reactor inlet and outlet were detected by light absorption. The detection unit consisted of a linear diode array detector (TSL, 1401R-LF) which had 128 diodes, each of dimensions 63.5 μm by 55.5 μm. Illumination was provided by two square LEDs (Kingbright L-15531DT). The line of 128 diodes in each sensor was positioned perpendicular to the flow direction so that only a certain number of diodes were under the tube. Using a Labview program, every 100 ms readings from the relevant diodes on each sensor were collected, averaged, and converted to a single absorbance measurement.

Analysis. Reaction analysis was carried out on a HP5890A gas chromatograph equipped with a Supelco SPB 1701 column (30 m × 0.32 mm, 0.25 μm), FID detector (injection port 250 °C, detector 250 °C, Oven initial 100 °C, final 180 °C hold for 2 min, 20 °C/min ramp); all product peaks (2 and 3) were referenced with authentic samples obtained from Sigma-Aldrich; spiked runs were also carried out. The GC relative peak areas were checked and found to be 1:1:1 when a 1:1:1 molar solution of 1, 2, and 3 was injected into the GC. No other 1-decene-derived products apart from 2 and 3 were observed in the GC trace, and thus, the total product peaks areas were assumed to equal unity. NMR spectra were run on a Bruker 400 MHz spectrometer in CDCl₃ and referenced to the residual solvent peak.

Decene 1: *R_f* (GC) 3.6 min; *R_f* (SiO₂, 10% EtOAc in cyclohexane) 0.75.

Nonanal 2: *R_f* (GC) 4.7 min; *R_f* (SiO₂, 10% EtOAc in cyclohexane) 0.5; δ_{H} (400 MHz, CDCl₃) 0.86 (3 H, t, *J* = 6.8, CH₃), 1.20–1.37 (10 H, m, 5 × CH₂), 1.62 (2 H, quin, *J* = 7.3 Hz, CH₂), 2.40 (2 H, td, *J* = 7.3, 1.9 Hz, CH₂) and 9.75 (1 H, t, *J* = 1.9 Hz, CHO).

Nonanoic Acid 3: *R_f* (GC) 6.8 min; δ_{H} (400 MHz, CDCl₃) 0.88 (3 H, t, *J* = 6.8, CH₃), 1.20–1.76 (12 H, m, 6 × CH₂), 2.33 (2 H, t, *J* = 7.5, CH₂) and 11.00 (1 H, br s, COOH).

3-Octyl-1,2,4-trioxolane (decene ozonide) 4: δ_{H} (400 MHz, CDCl₃) 0.81 (3 H, t, *J* = 6.6, CH₃), 1.10–1.30 (10 H, m, 5 × CH₂), 1.32–1.41 (2 H, m, CH₂), 1.61–1.68 (2 H, m, CH₂), 4.95 (1H, s, OCH_AH_BO), 5.05 (1H, t, *J* = 4.9, CH) and 5.11 (1 H, s, OCH_AH_BO).

RESULTS

Hydrodynamics Characterization. Figure 2 shows the observed flow patterns for different liquid (ethyl acetate) to gas (nitrogen) flow rate ratio: (a) slug-annular (1:17, $V_{\text{liquid}} = 1.5 \text{ mL min}^{-1}$, $V_{\text{gas}} = 25 \text{ mL min}^{-1}$), (b) wavy annular (1:33, $V_{\text{liquid}} = 0.75 \text{ mL min}^{-1}$, $V_{\text{gas}} = 25 \text{ mL min}^{-1}$), (c) wavy annular (1:100, $V_{\text{liquid}} = 0.25 \text{ mL min}^{-1}$, $V_{\text{gas}} = 25 \text{ mL min}^{-1}$), and annular flow (1:400, $V_{\text{liquid}} = 0.25 \text{ mL min}^{-1}$, $V_{\text{gas}} = 100 \text{ mL min}^{-1}$). For the liquid to gas flow rate ratio of (1:17) slug annular flow is observed as an intermediate flow pattern between slug and annular flow. In this regime the gas slugs are large and are separated by a thin bridge (Figure 2a). Decreasing the liquid to gas flow rate ratio leads to the disappearance of the bridge and the appearance of waves. This constitutes the wavy annular flow regime (Figure 2b and c) which persists up to liquid to gas flow rate ratios of 1:300.

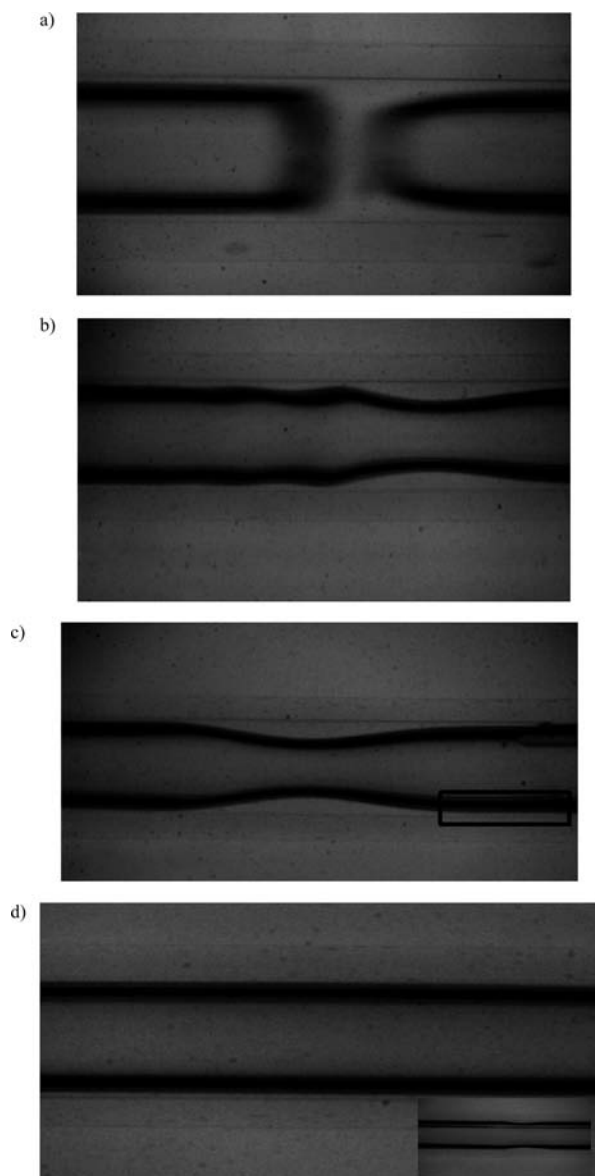


Figure 2. Flow patterns observed in 1 mm ID PFA tubing for various ethyl acetate/nitrogen volumetric flow rate ratios. (a) Slug-annular (1:17), (b) wavy annular (1:33), (c) wavy annular (1:100), and (d) annular flow (1:400).

Further decrease of the ratio leads to annular flow (Figure 2d). This flow pattern is quite stable, but very rarely waves appear as can be seen in the inset picture. In wavy annular and annular flow the liquid film flows on the tube wall, and continuous gas flows in the tube core. Furthermore, from Figure 2 it can be seen that waves tend to attenuate when the liquid to gas ratio decreases. Similar flow-patterns have been reported in the literature.^{19,14} The major parameters that affect the flow patterns and wave formation are fluid flow rates, wall wetting properties, tube diameter, and surface tension.¹⁴ In our case only the liquid and gas flow rates are altered and hence are the key parameters for wave formation and removal. The liquid film thickness was extracted from the images (within the rectangular area, see Figure 2c), by using a pixel counting technique and it was found to be in the range of 40–60 μm in the wavy annular flow. This thickness does not account for the waves which were 200–300 μm thick at their maximum. Similar film thicknesses were observed

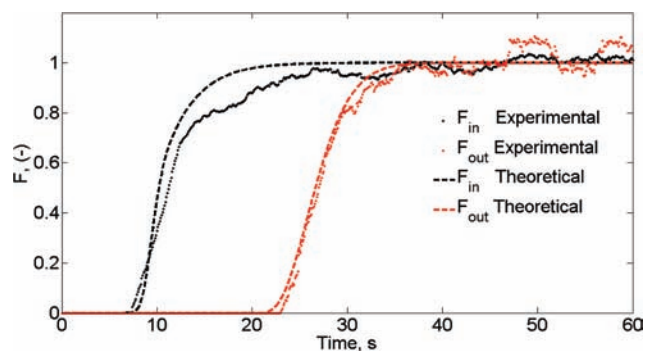


Figure 3. Cumulative age distribution function, F , at reactor inlet and outlet obtained during a step-input tracer experiment in a 2-mL coil, where nitrogen/ethyl acetate flowed. $V_{\text{gas}} = 50 \text{ mL min}^{-1}$, $V_{\text{liquid}} = 0.25 \text{ mL min}^{-1}$. Theoretical curves are obtained by fitting the experiments to a model of axial dispersion exchanging mass with a stagnant zone.

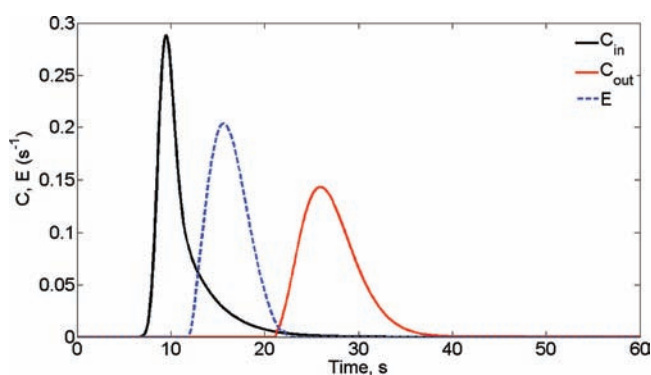


Figure 4. Reactor inlet and outlet age distributions curves, C , obtained by fitting tracer step-input experiments to a model of axial dispersion exchanging mass with a stagnant zone. The corresponding residence time distribution, E , is also shown.

for two-phase air–water flow in horizontal circular microchannels of 0.53 mm ID.¹⁹ In the ozonolysis experiments the liquid to gas flow rate ratio was in the order of 1:100. At these conditions the flow pattern was wavy annular, with some droplets occasionally flowing through the gas core.

An example of the results of a step-input experiment, in terms of the dimensionless tracer signals (or cumulative age distribution functions, F), for liquid residence time distribution (RTD) determination is shown in Figure 3. Experimental results were fitted to a model of axial dispersion exchanging mass with a stagnant zone (ADEM). The model parameters calculated from the fitting were used to obtain age distribution curves for the inlet and outlet tracer signals. Fitting of the tracer experiments was employed because deconvolution from raw experimental data resulted in noisy curves that were unsatisfactory and could not be improved by signal filtering or curve smoothing. The RTD shown in Figure 4, was obtained by deconvoluting the output age distribution curve from the input one. This RTD indicates that the reactor behaviour is close to plug flow with only a small level of dispersion. A simple axial dispersion model provided a vessel dispersion number ($D_{\text{ax}}/(\nu L)$) (where D_{ax} is the axial dispersion coefficient, ν is the fluid velocity and L is the reactor length) of ~ 0.01 , which is also consistent with negligible dispersion.²⁰ It must be pointed out though that the fit was not as good as that from the ADEM model.

More details of the procedure to fit experimental RTD data to the ADEM model can be found in Perez et al.²¹

Table 2 shows the results of the tracer experiments at different operating conditions. The mean residence time in this case was obtained experimentally from the difference between the inlet and outlet signals of the times when the tracer concentration was 50% of the final values. The mean residence time was also obtained from the fitted RTDs (for selected cases of Table 2) and it was within 5% of the experimental ones. Differences can be attributed to the fact that the fitting does not reproduce exactly the experimental graphs. The residence time showed a direct dependency to the volumetric liquid flow rate, while an increase in the gas flow rate only had a slight effect on the measurements when the liquid flow was kept constant. When the liquid flow rate doubled, the residence time decreased to about half.

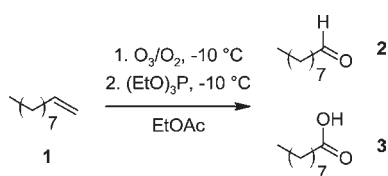
Reaction Experiments. Initial studies were carried out using *n*-decene (0.2–0.4 M in EtOAc) as the substrate and triethylphosphite (0.3–0.6 M in EtOAc) as the quench (Scheme 1).

In initial experiments flow rates were *n*-decene **1** (0.2 M) 0.25 mL min⁻¹, (EtO)₃P (0.3 M) 0.25 mL min⁻¹, and O₂/O₃

Table 2. Experimentally measured liquid mean residence times in ozonolysis reactors

reactor coil [mL]	reactor length [mm]	V (gas) [mL min ⁻¹]	V (liquid) [mL min ⁻¹]	mean residence time of liquid [s]
2	2546	25	0.25	18.5
2	2546	25	0.50	9.1
2	2546	50	0.25	18.4
2	2546	50	0.50	8.8
5	6366	25	0.25	38.0
5	6366	25	0.50	19.2
5	6366	50	0.25	34.2
5	6366	50	0.50	18.4
10	12732	25	0.25	81.5
10	12732	25	0.50	43.1

Scheme 1



25 mL min⁻¹. Using a 10-mL reactor coil, 2.4 equiv of ozone was sufficient to completely consume all *n*-decene, resulting in a 2:1 mixture of **2** and **3** as detected by GC (entry 1, Table 3). If the flow rates of the liquid reactant streams were doubled while keeping the O₂/O₃ flow the same, thus halving the equivalents of ozone, a small amount of **1** remained unconsumed (entry 2, Table 3). When the liquid flow rates remained the same but the reactant concentrations were doubled, no decene was detected (entry 3, Table 3). To further look at the stoichiometry of the reaction, a run was carried out using only 0.7 equiv of ozone, resulting roughly in a 1:1 mixture of the starting material **1** and the products **2** and **3** (entry 4, Table 3). This result points towards an ideal amount of ozone as being ~1.2 equiv.

The literature suggests that the reaction of ozone with alkenes is mass transfer controlled, and therefore, efficient gas–liquid mixing and mixing time are very important.^{9–12,22} The reactor volume was reduced to 2 mL to determine the minimum needed. Using the standard conditions, no decene was detected by GC when using a 2-mL reactor (entry 5, Table 3). Again no decene was found when only 1.5 equiv of ozone (achieved by adjusting the power setting on the ozoniser) was used in conjunction with a 2-mL coil (entry 7, Table 3). Even when the reactor volume was reduced to 0.07 mL (10 cm long 1.0 mm ID tube), no decene was seen (entry 8, Table 3). The expected liquid residence time for the 0.07-mL volume reactor is ~1 s based on a linear extrapolation of the data in Table 2. In all these runs the ratio of desired aldehyde **2** to undesired acid **3** was approximately 2:1. It was first thought that the aldehyde in the gas/liquid separator was being oxidised by an O₂/O₃ mixture. To test this the gas–liquid output from the ozonolysis reactor was “diluted” with N₂ (100 mL min⁻¹), but no change to the ratio was seen (entry 6, Table 3). If a solution of excess triethylphosphite (1.5 equiv) is ozonised, no ozone is detected in the output gas, demonstrating that no ozone should be present in the off-gas when the equivalents of phosphite are greater than the equivalents of ozone. When the solution collected in the gas/liquid separator was sampled immediately following a run, ¹H NMR analysis revealed the presence of unquenched ozonide, which implied that the phosphite was unable to completely reduce the ozonide products within the time frame of the fast flow process. This ozonide is not observed via gas chromatography, presumably because of thermolysis to the corresponding acid and aldehyde as seen previously by Steinfeldt et al.¹¹ These results indicated that, while the reaction of the ozone with the alkene is very efficient and fast under flow conditions, the subsequent quench with triethylphosphite is not.

Table 3. Ozonolysis of decene using triethylphosphite as quench in EtOAc at -10 °C^a

entry	decene			EtO ₃ P			O ₂ /O ₃			reactor vol.(mL)	relative amounts		
	mL min ⁻¹	conc. (M)	equiv	mL min ⁻¹	conc. (M)	equiv	mL min ⁻¹	conc. (M)	equiv		2 ^b	3 ^b	1 ^b
1	0.25	0.2	1.0	0.25	0.3	1.5	25	0.0048	2.4	10	1.0	0.5	ND
2	0.50	0.2	1.0	0.50	0.3	1.5	25	0.0048	1.2	10	1.0	0.4	0.2
3	0.25	0.4	1.0	0.25	0.6	1.5	25	0.0048	1.2	10	1.0	0.5	ND
4	0.50	0.4	1.0	0.50	0.6	1.0	25	0.0056	0.7	10	1.0	0.3	1.2
5	0.25	0.2	1.0	0.25	0.3	1.5	25	0.0044	2.2	2	1.0	0.50	ND
6 ^c	0.25	0.2	1.0	0.25	0.3	1.5	25	0.0048	2.4	2	1.0	0.50	ND
7	0.25	0.2	1.0	0.25	0.3	1.5	25	0.0030	1.5	2	1.0	0.42	ND
8	0.25	0.2	1.0	0.25	0.3	1.5	25	0.0030	1.5	0.07	1.0	0.34	ND

^a All runs were carried out for 5 min. ^b GC ratios referenced to nonanal **2**. ^c N₂ (100 mL min⁻¹) used to dilute output gas stream.

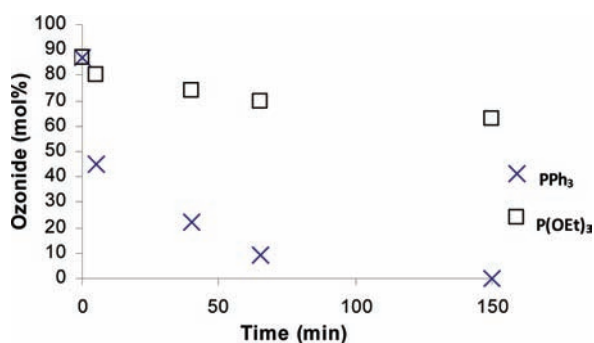
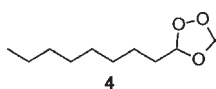


Figure 5. Reduction of decene ozonide **4** as a function of time with both triphenylphosphine and triethylphosphite at 20 °C, in batch mode.

Considering the mean residence times results of Table 2, the ozonolysis experiments reported in Table 3 correspond to liquid residence time in the ozonolysis reactor of 1–80 s. Entry 2 (Table 3) corresponds to residence time ~ 40 s, while entry 8 corresponds to ~ 1 s. However, complete substrate conversion was observed only for the latter. This may be due to the system pressure and, hence, the flow/mixing pattern. With a 10-mL coil the pattern was not as smooth as in a smaller coil, which had a small back pressure. This problem with back-pressure and inconsistent flow pattern also limits the quench reactor size and thus the residence time.

The literature shows that, in the case of the reduction of styrene ozonide to benzaldehyde by both triethyl phosphite²³ and triphenylphosphine,²⁴ the rate of reduction by triphenylphosphine ($6.6 \times 10^{-2} \text{ L mol}^{-1} \text{ s}^{-1}$) is over an order of magnitude faster than triethylphosphite ($2.2 \times 10^{-3} \text{ L mol}^{-1} \text{ s}^{-1}$). To see if this was the case in our system, a solution of decene ozonide was prepared in flow. ¹H NMR analysis of the mixture showed a $\sim 8:1$ ratio of ozonide:aldehyde without addition of a quench reagent, this ratio was stable for at least 24 h. The solution was then split into two equal portions. To one portion was added, in one go, 2.0 equiv of triphenylphosphine and to the other was added 2.0 equiv of triethylphosphite. Both portions were given a quick stir and then left to stand for 5 min. Samples (10 drops) were mixed with CDCl₃ and analysed by ¹H NMR. Samples were then taken after 40, 65, and 150 min. The results are shown in Figure 5. The data clearly show that in the case of decene ozonide **4**, as with styrene ozonide, triphenylphosphine is a much more effective reductant than triethylphosphite. The quenching by triphenylphosphine in this limited kinetic study seems to be slower than during flow (*vide infra*). It is observed that the time taken for half the initial concentration of ozonide to be reduced is ~ 5 min, but for it to be reduced by half again takes a further 35 min. This may suggest a change in mechanism and/or substrate being reduced. The difference between the flow and kinetic study quench times (~ 10 vs ~ 15 min) could be because of the age of the ozonide sample. In the case of the kinetic study, polymeric ozonides and/or stable molecular clusters could be present, which would be more difficult to reduce.



Given that triphenylphosphine is a more potent reducing agent, a 0.3 M solution was prepared and a run carried out with initially 3 equiv (entry 1, Table 4). A significant reduction in the

amount of acid **3** was observed, which corresponded to a more active quench. If the level of PPh₃ was dropped down to 2 equiv, then a rise in the acid level was seen (entry 2, Table 4). This can be rationalised by the fact that ozone can easily oxidise the phosphine and thus leaving less available to quench the produced ozonides. Therefore, the ozone level was then sequentially dropped to 1.5–1.8 equiv, by adjusting both the substrate flow rate and the ozoniser power setting, to result in similarly low levels of acid **3**, albeit with a small amount of unreacted decene (entries 3 and 4, Table 4). A larger 2-mL reactor was employed to achieve complete consumption of **1** (entry 5, Table 4). A small rise in the level of **3** was remedied by the reduction of the ozone equivalents to 1.25 (entry 6, Table 4). Doubling all the flow rates and thus the production per unit time resulted in similarly good results (entry 7, Table 4). The addition of a 5-mL quench reactor after the introduction of the quench stream did not change the outcome (entry 8, Table 4), indicating that the standard 0.393-mL quench reactor gave more than sufficient time for the quench to occur.

It was also discovered during the course of the study that an important factor for reproducibility was the stability of the reactor flow pattern and thus mixing. It was found that, along with visual observation, a good indicator of a stable flow pattern was the O₂/O₃ input line pressure (measured at the ozone analyser), with steady (± 5 mbar) pressure being associated with good selectivity and repeatability.

A study was carried out to determine the equivalents of ozone needed in batch to totally consume the starting materials. Five milliliters of a 0.2 M solution of decene was placed in a flask and ozone passed through the solution using a 1.0 mm ID tube for a defined amount of time resulting in differing equivalents of ozone (Table 5). After each run, when the flow of ozone had ceased, a sample was taken and analysed by GC to determine the level of starting material left. In all runs complete consumption of the starting material was observed except when 1.08 equiv was used (entry 1, Table 5). One important observation was that the levels of the analogous acid **3** increased (detected by GC) as addition of ozone increased (entries 1–7, Table 5). It is assumed that when the sample is injected into the GC injection port at 250 °C the ozonide **4** is thermally decomposed to two possible sets of compounds, either nonanal **2** and formic acid or nonanoic acid **3** and formaldehyde.¹¹ Therefore, it is expected that a solution of **4** in a particular solvent will always thermally fragment in the same way to the same extent.

Several samples of **4** previously prepared using the flow apparatus (decene 0.2 M, 0.25 mL min⁻¹, 5 min; ozone 0.0036 M, 25 mL min⁻¹, 1.25–1.9 equiv; EtOAc) were injected into the GC to give aldehyde/acid ratios of 2:1 to 3:1, indicating the preferred thermal breakdown pathway of **4** results in nonanal and formic acid. Given this analysis, it was surprising to see an ozone equivalence dependency of the acid levels. An explanation for this is that the excess ozone reacts with the secondary ozonide, resulting in overoxidation. This is a plausible explanation, as ozone is known to react with cyclic acetals.²⁵ When a larger-scale batch ozonolysis was carried out comparable results were obtained (entry 8, Table 5). At -78 °C the absorption of ozone appears less efficient, resulting in a higher amount of unreacted **1** (entry 9, Table 5). This result emphasises the advantages of flow over batch as ozonolysis in flow can be safely performed at room temperature as there are safety issues with batch at room temperature on a large scale. The conditions in entry 1, Table 5 were repeated as closely as possible under flow conditions (**1** 0.2 M, 0.54 mL min⁻¹, 5 min, 0.54 mmol; ozone 0.0037 M, 33 mL min⁻¹, 5 min,

Table 4. Ozonolysis of decene using triphenylphosphine as quench in EtOAc at -10°C

entry	decene			Ph_3P			O_2/O_3			reactor vol.(mL)	relative amounts		
	mL min^{-1}	conc. (M)	equiv	mL min^{-1}	conc. (M)	equiv	mL min^{-1}	conc. (M)	equiv		2 ^a	3 ^a	1 ^a
1	0.25	0.2	1.0	0.50	0.3	3.0	25	0.0052	2.6	0.07	1.0	0.02	ND
2	0.25	0.2	1.0	0.33	0.3	2.0	25	0.0052	2.6	0.07	1.0	0.22	ND
3	0.25	0.2	1.0	0.33	0.3	2.0	25	0.0036	1.8	0.07	1.0	0.04	ND
4	0.30	0.2	1.0	0.40	0.3	2.0	25	0.0036	1.5	0.07	1.0	0.04	0.02
5	0.30	0.2	1.0	0.40	0.3	2.0	25	0.0036	1.5	2	1.0	0.13	ND
6	0.36	0.2	1.0	0.48	0.3	2.0	25	0.0036	1.25	2	1.0	0.04	ND
7	0.72	0.2	1.0	1.44	0.3	2.5	50	0.0036	1.25	2	1.0	0.02	ND
8 ^b	0.72	0.2	1.0	1.44	0.3	2.5	50	0.0036	1.25	2	1.0	0.03	ND

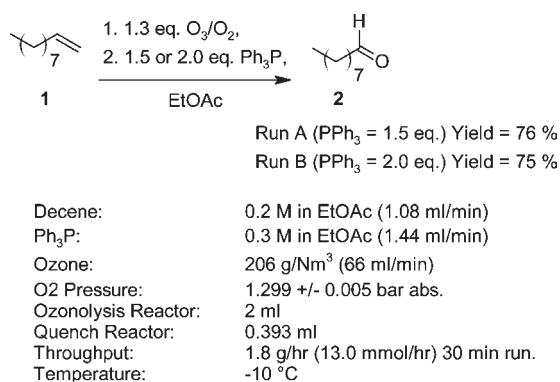
^a GC ratios referenced to nonanal 2. ^b 5 mL residence coil added after quench T-junction.

Table 5. Decene 2 consumption with increasing ozone equivalents using a 0.2 M solution in batch

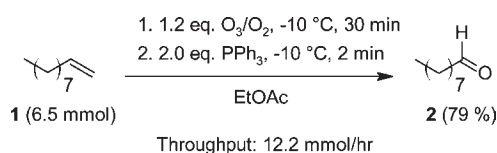
entry	0.2 M decene		0.0035 M ozone		temperature ($^{\circ}\text{C}$)	decene remaining ^a	acid detected ^a
	(mL)	[60 mL min^{-1} (equiv)]	[60 mL min^{-1} (equiv)]	[60 mL min^{-1} (equiv)]			
1	5	1.08	20	0.08	20	0.25	
2	5	1.30	20	0	20	0.30	
3	5	1.52	20	0	20	0.44	
4	5	1.70	20	0	20	0.45	
5	5	1.86	20	0	20	0.48	
6	5	3.17	20	0	20	0.49	
7	5	6.75	20	0	20	0.86	
8	20	1.05	20	0.05	20	0.17	
9	5	1.05	-78	0.34	20	0.14	

^a Ratio, compared to nonanal (1.0).

Scheme 2. Flow process carried out in the Vapourtec module with 2-mL reactor



Scheme 3. Batch process carried out in a 50-mL round-bottom flask



0.61 mmol, 1.1 equiv; 2-mL reactor, 20°C , EtOAc) to give very little decene (0.04 in relation to 2) and only 0.1 of 3 in relation to 2. After addition of 2 equiv of PPh_3 this level was reduced to below 0.01.

After optimisation and refinement of the flow procedure, several larger-scale experiments were carried out with total run times of 30 min. Two runs in flow were carried out (Scheme 2), the first being with 1.5 equiv of triphenylphosphine as quench (run A) and the other with 2.0 equiv (run B). In both cases good yields of 76% and 75% of nonanal 2 were obtained. These yields were comparable to that obtained (79%) with an identical batch experiment (Scheme 3). The less than excellent yields are associated with a problematic work up due to the difficulty of removing the triphenylphosphine waste product. A space time yield of $6.5 \text{ mmol cm}^{-3} \text{ h}^{-1}$ compares favorably with that achieved by Wada et al. in a multichannel microreactor with posts ($18.9 \text{ mmol cm}^{-3} \text{ h}^{-1}$), considering the simple nature of coiled tubing.⁹ Even though the throughput of both flow and batch systems is similar ($12.2\text{--}13 \text{ mmol h}^{-1}$), the space time yield of the batch system, $0.24 \text{ mmol cm}^{-3} \text{ h}^{-1}$, is smaller because of its larger volume (50 cm^3). With further work the productivity of the flow system could be improved with the right balance of gas flow rates, liquid flow rates, and reagent concentrations, while keeping in mind the pressure limitations of the ozone analyser (maximum 2 bar abs.). We have noticed that, if the liquid flow rate or the viscosity is too high, the flow pattern switches to slug flow with a subsequent unacceptable rise in the back pressure of the reactor. This can be alleviated by increasing the gas flow, but there is a limit to this. The major advantage compared to the batch process is the ability to process a large amount of material in a safe, controlled manner without the build-up of dangerous ozonides.

CONCLUSIONS

The ozonolysis of 1-decene 1 has been demonstrated using a commercially available ozoniser and a Vapourtec flow system. The flow pattern observed in the reactor channels was found to be annular albeit strongly wavy in fashion. Liquid experimental residence times were observed to be independent of the gas flow rates within the conditions considered, while residence time distribution measurements indicated only a small level of dispersion. Triphenylphosphine was demonstrated to be a more viable quench than triethylphosphite due to its higher activity. Higher temperatures (-10°C) were used in the flow system than typical for a batch process (-78°C), therefore allowing for an energy efficient process for scale-up without the safety concerns associated

with large-scale batch ozonolysis. Experiments under equivalent conditions with a batch reactor showed similar nonanal 2 throughput (12.2–13 mmol h⁻¹), but the space time yield of the flow system was much larger because of its smaller reactor volume.

AUTHOR INFORMATION

Corresponding Author

*Telephone: +44 (0)20 7679 3811. Fax: +44 (0)20 73832348.
E-mail: a.gavriilidis@ucl.ac.uk.

ACKNOWLEDGMENT

Funding from EPSRC, GSK, and Pfizer is gratefully acknowledged.

REFERENCES

- (1) Bailey, P. S. *Chem. Rev.* **1958**, 925.
- (2) Hoigné, J. In *Handbook of Environmental Chemistry*; Hrubec, J., Ed. Springer-Verlag: Berlin, 1998; Vol. 5, part C, pp 83–141.
- (3) Criegee, R. *Angew. Chem., Int. Ed. Engl.* **1975**, 14, 745.
- (4) Thomson, Q. E. *J. Am. Chem. Soc.* **1961**, 83, 846.
- (5) Sahle-Demessie, E.; Devulapelli, V. G. *Appl. Catal., B* **2008**, 84, 408.
- (6) Rice, R. G., Netzer, A., Eds. *Handbook of Ozone Technology and Applications*; Butterworth: Boston, 1984; Vol. 2.
- (7) (a) Hill, R. H., Jr.; Nelson, D. A. Strengthening safety education of chemistry undergraduates. In *Chemical Health & Safety* **1999**, (November/December), 21. (b) Dyer-Smith, P.; Heiniger, B.; Jenny, R. <http://www.io3s.com/english/ozone/publications/index.html>, December 2004. (c) <http://www.icis.com/Articles/2003/08/13/511874/explosion-injures-18-at-dsm-fine-chems-plant-in-linz-austria.html>.
- (8) (a) Kiwi-Minsker, L.; Renken, A. *Catal. Today* **2005**, 110, 2. (b) Hessel, V.; Angeli, P.; Gavriilidis, A.; Löwe, H. *Ind. Eng. Chem. Res.* **2005**, 44, 9750. (c) Jähnisch, K.; Hessel, V.; Löwe, H.; Baerns, M. *Angew. Chem., Int. Ed.* **2004**, 43, 406. (d) Günther, A.; Jensen, K. F. *Lab Chip* **2006**, 6, 1487.
- (9) Wada, Y. W.; Schmidt, M. A.; Jensen, K. F. *Ind. Eng. Chem. Res.* **2006**, 45, 8036.
- (10) Steinfeld, N.; Abdallah, R.; Dingerdissen, U.; Jähnisch, K. *Org. Process Res. Dev.* **2007**, 11, 1025.
- (11) Steinfeldt, N.; Bentrup, U.; Jähnisch, K. *Ind. Eng. Chem. Res.* **2010**, 49, 72.
- (12) Hübner, S.; Bentrup, U.; Budde, U.; Lovis, K.; Dietrich, T.; Freitag, A.; Küpper, L.; Jähnisch, K. *Org. Process Res. Dev.* **2009**, 13, 952.
- (13) O'Brien, M.; Baxendale, I. R.; Ley, S. V. *Org. Lett.* **2010**, 12, 1596.
- (14) Shao, N.; Gavriilidis, A.; Angeli, P. *Chem. Eng. Sci.* **2009**, 64, 2749.
- (15) Hall-Taylor, G. F.; Hewitt, P. M.; Lacy, C. *Chem. Eng. Sci.* **1963**, 18, 537.
- (16) Saisorn, S.; Wongwises, S. *Exp. Therm. Fluid Sci.* **2010**, 34, 454.
- (17) Moeck, E. O.; Stachiewicz, J. W. *Int. J. Heat Mass Transfer* **1972**, 15, 637.
- (18) Lopes, J. B. C.; Dukler, A. E. *AIChE J.* **1986**, 32, 1500.
- (19) Saisorn, S.; Wongwises, S. *Exp. Therm. Fluid Sci.* **2008**, 32, 748.
- (20) Levenspiel, O. *Chemical Reaction Engineering*; 3rd ed.; John Wiley & Sons, New York, 1999.
- (21) Perez, C. A.; Barras, S.; Gavriilidis, A. *Chem. Eng. J.* **2010**, 160, 834.
- (22) Razumovskii, S. D.; Zaikov, G. E. *Russ. Chem. Rev.* **1980**, 49, 1163.
- (23) Carles, J.; Fliszár, S. *Can. J. Chem.* **1972**, 50, 2552.
- (24) Carles, J.; Fliszár, S. *Can. J. Chem.* **1970**, 48, 1309.
- (25) Deslongchamps, P.; Atlani, P.; Fréhel, D.; Malaval, A.; Moreau, C. *Can. J. Chem.* **1974**, 52, 3651.

NOTE ADDED AFTER ASAP PUBLICATION

This paper was published on the Web on July 7, 2011, with an error in the second paragraph of the Introduction. The corrected version was reposted on July 18, 2011.